Int. J. Heat Mass Transfer. Vol. 32, No. 11, pp. 2135–2148, 1989
Printed in Great Britain

0017–9310/89 $3.00+0.00

Non-Darcian effects on natural convection in a vertical porous enclosure

G. LAURIAT†
University of Nantes, 44072 Nantes Cedex 02, France

and

V. PRASAD
Department of Mechanical Engineering, Columbia University, New York, NY 10027, U.S.A.

(*Received* 4 *January and in final form* 24 *March* 1989)

Abstract—The relative importance of inertia and viscous forces on natural convection in porous media is examined via the Darcy–Brinkman–Forchheimer solutions for a differentially heated vertical cavity. These results indicate that there exists an asymptotic convection regime where the solution is independent of the permeability of the porous matrix, or the Darcy (*Da*) and Forchheimer (*Fs*) numbers. The higher the fluid Rayleigh number, *Ra*, the earlier this regime starts in terms of *Da* and *Fs*. In this convective state, not only the average Nusselt number but also the temperature and flow fields for a fixed *Ra* match with the fluid results provided the conductivity ratio for the porous medium is unity. Otherwise, the Nusselt number always increases with the fluid Rayleigh number, the Darcy number and the conductivity ratio while $\overline{Nu}$ decreases when *Fs* increases. The effect of Prandtl number is not straightforward, and depends on the flow regime and other parameters. The numerical solutions further indicate that it is possible that a porous medium can transport more energy than a saturating fluid alone if the porous matrix is highly permeable and the thermal conductivity of solid particles is greater than that for the fluid. Several criteria to delimit the various convective flow regimes are also presented for a square cavity.

1. INTRODUCTION

NON-DARCY effects on natural convection in porous media have received a great deal of attention in recent years because of the experiments conducted with several combinations of solids and fluids covering wide ranges of governing parameters which indicate that the experimental data for systems other than glass–water at low Rayleigh numbers, do not agree with the theoretical predictions based on the Darcy flow model. This divergence in the heat transfer results has been reviewed in detail in Cheng [1] and Prasad *et al.* [2] among others. Extensive efforts are thus being made to include the inertia and viscous diffusion terms in the flow equations and to examine their effects in order to develop a reasonable accurate mathematical model for convective transport in porous media. Detailed accounts of the recent efforts on non-Darcy convection have been recently reported in Tien and Hong [3], Cheng [4], Prasad *et al.* [5], and Kladias and Prasad [6]. Here, we will restrict our discussion to the vertical cavity only.

Poulikakos and Bejan [7, 8] investigated the inertia effects through the inclusion of Forchheimers's velocity-squared term, and presented the boundary layer analyses for tall cavities. They also obtained numerical results for a few cases in order to verify the accuracy of their boundary layer solutions. Later, Prasad and Tuntomo [9] reported an extensive numerical work for a wide range of parameters, and demonstrated that the effects of Prandtl number remain almost unaltered while the dependence on the modified Grashof number, Gr^*, changes significantly with an increase in the Forchheimer number. This results in a reversal of flow regimes from boundary layer to asymptotic to conduction as the contribution of the inertia term increases in comparison with that of the boundary term. They also reported a criterion for the Darcy flow limit.

The Brinkman–extended Darcy model was considered in Tong and Subramanian [10], and Lauriat and Prasad [11] to examine the boundary effects on free convection in a vertical cavity. While Tong and Subramanian performed a Weber-type boundary layer analysis, Lauriat and Prasad solved the problem numerically for $A = 1$ and 5. It was shown that for a fixed modified Rayleigh number, Ra^*, the Nusselt number decreases with an increase in the Darcy number; the reduction being larger at higher values of Ra^*. A scale analysis as well as the computational data also showed that the transport term $(\mathbf{V}\cdot\nabla)\mathbf{V}$, is of low order of magnitude compared to the diffusion plus buoyancy terms [11].

A numerical study based on the Forchheimer–Brinkman–extended Darcy equation of motion has also been reported recently by Beckermann *et al.* [12]. They demonstrated that the inclusion of both the inertia and boundary effects are important for convection

† Present address: Laboratoire de Thermique, CNAM, 292 rue Saint-Martin, 75141 Paris Cedex 03, France.

NOMENCLATURE

A	aspect ratio, H/D
b	matrix structure property associated with the Forchheimer term [m]
C	constant in the Ergun model
c	specific heat at constant pressure [J kg^{-1} K^{-1}]
d	characteristic particle dimension [m]
D	width of cavity [m]
Da	Darcy number, equation (9)
f	ψ, Ω or θ in equation (18)
Fs	Forchheimer number, equation (10)
$\mathbf{g}$	body force vector
g	acceleration due to gravity [m s^{-2}]
Gr	fluid Grashof number, $g\beta D^3\Delta T/\nu^2$
Gr^*	Darcy–Grashof number, $g\beta KD\Delta T/\nu^2$
H	height of cavity [m]
$\mathbf{k}$	unit vertical vector
k_f	fluid thermal conductivity [W m^{-1} K^{-1}]
k_m	stagnant thermal conductivity of porous medium [W m^{-1} K^{-1}]
K	permeability of porous matrix [m^2]
Nu	local Nusselt number based on k_m
$\overline{Nu}$	average Nusselt number based on k_m
p	pressure [Pa]
P	dimensionless pressure
Pr	fluid Prandtl number, equation (8)
Pr^*	Prandtl number for porous media, ν/α_m
Ra	fluid Rayleigh number, equation (7)
Ra^*	Darcy–Rayleigh number, $g\beta KD\Delta T/\nu\alpha_m$
S	specific heat ratio, equation (13)
t	dimensionless time
$\underline{t}$	time [s]
T	temperature [K]
T_0	average temperature, $(T_h+T_c)/2$ [K]
ΔT	temperature difference, (T_h-T_c) [K]
u, v	dimensionless velocity components
$\underline{\mathbf{V}}$	velocity vector [m s^{-1}]
$\mathbf{V}$	dimensionless velocity vector
x, y	dimensionless coordinates.

Greek symbols

α_f	thermal diffusivity of fluid [m^2 s^{-1}]
α_m	thermal diffusivity of porous medium, $k_m/(\rho c)_f$, [m^2 s^{-1}]
β	isobaric coefficient of thermal expansion of fluid [K^{-1}]
γ	dimensionless particle diameter
ε	porosity
θ	dimensionless temperature
λ	conductivity ratio, k_f/k_m
Λ	viscosity ratio, μ'/μ
μ_f	dynamic viscosity of fluid [kg m^{-1} s^{-1}]
μ'	apparent viscosity for Brinkman's model [kg m^{-1} s^{-1}]
ν	kinematic viscosity of fluid [m^2 s^{-1}]
ξ	vorticity
ρ	density [kg m^{-3}]
ψ	stream function.

Subscripts

c	cooled wall
f	fluid
h	hot wall
m	fluid-saturated porous medium
w	wall.

in a rectangular packed-sphere cavity. The importance of considering the Rayleigh number, $Ra = \lambda Ra_f$, and the Darcy number, Da, was also recognized in this work. However, they considered the Forchheimer number as a known function of Darcy number, $Fs = 0.55Da^{0.5}$, which is applicable for the Ergun model only with $\varepsilon \cong 0.4$. They also presented correlations for three ranges of parameters.

The purpose of the present work is to re-examine the significance of both Forchheimer and Brinkman's modifications to the Darcy model on free convection in a vertical porous cavity. It is shown that the Darcy–Brinkman solutions (for $k_f = k_s$) approach the fluid results beyond the Darcy flow limit. Strong arguments are thus advanced in favor of a dimensional analysis which leads to:

(a) the flow parameters: fluid Rayleigh (or Grashof) and Prandtl numbers;

(b) the porous matrix scaling parameters: porosity, Darcy and Forchheimer numbers;

(c) the combined parameters: conductivity, viscosity and specific heat ratios as complex functions of the solid and fluid properties.

Considerations of these parameters help in establishing the true effects of the Darcy number, that is, the heat transfer rate increases with the Darcy number or the permeability of the porous matrix. It will be demonstrated that the Nusselt vs Darcy number plot is an asymptotic curve, indicating that the energy transport is independent of the porous matrix structure in the asymptotic convection regime. Another important property which will be recognized here is that a porous medium can transport significantly larger amounts of energy compared to the corresponding fluid alone provided the porous matrix is highly permeable, and the solid particles are more heat conducting than the fluid ($k_s > k_f$).

2. MATHEMATICAL FORMULATION

Since the flow through porous media deviates from the Darcian behavior at a particle Reynolds number,

Re, greater than unity, it has long been argued that a higher-order model be considered under such conditions, i.e. at high velocities. As noted in previous studies, Forchheimer's second-order equation for the filtration velocity seems to be the best choice for laminar non-Darcy flow in porous media, $1 < Re < 100$, since most of the non-linear equations reported in the literature are similar to the Forchheimer equation. The coefficients in this equation then depend on the particle size, d, the porosity, ε, the shape factor and so-forth, depending on the conceptual model being considered.

Brinkman's modification to the Darcy equation of motion has not been considered to be important by the porous media researchers except in the case of sparsely packed beds, primarily because the drag introduced by the boundary is generally small compared to that due to the ensemble of solid particles. However, since the convective heat transfer is mostly a boundary phenomenon, this modification to include the viscous diffusion effects can be of great importance to the energy transport processes.

For an isotropic, homogeneous, fluid-saturated porous medium, the governing equations which include both the Forchheimer and Brinkman modifications may be written as

$$\nabla \cdot \underline{\mathbf{V}} = 0 \tag{1}$$

$$\frac{\rho_f}{\varepsilon}\frac{\partial \underline{\mathbf{V}}}{\partial t} + \frac{\rho_f}{\varepsilon^2}(\underline{\mathbf{V}}\cdot\nabla)\underline{\mathbf{V}} = -\nabla p + \rho_f \mathbf{g} - \frac{\mu_f}{K}\underline{\mathbf{V}} - \frac{\rho_f b}{K}|\underline{\mathbf{V}}|\underline{\mathbf{V}} + \mu'\nabla^2\underline{\mathbf{V}} \tag{2}$$

$$(\rho c)_m \frac{\partial T}{\partial t} + (\rho c)_f(\underline{\mathbf{V}}\cdot\nabla)T = k_m \nabla^2 T. \tag{3}$$

Here, the thermophysical properties of the solid and fluid have been assumed to be constant except for the density variation in the body force term (Boussinesq approximation), and the solid particles and fluid are considered to be in local thermal equilibrium. The values of K and b depend on the model used to represent the Darcy–Forchheimer equation (refer to Bear [13] for their values). The apparent viscosity μ' in equation (2) may have a different value than the fluid viscosity [14].

Equations (1)–(3) may be rendered dimensionless by employing the following scales: D for length; D^2/α_m for time; α_m^4/K for pressure; α_m/D for velocity; and $(T_h - T_c)$ for temperature. We obtain

$$\nabla \cdot \mathbf{V} = 0 \tag{4}$$

$$\frac{Da}{\lambda Pr}\left[\frac{1}{\varepsilon}\frac{\partial \mathbf{V}}{\partial t} + \frac{1}{\varepsilon^2}(\mathbf{V}\cdot\nabla)\mathbf{V}\right] = -\nabla P + \lambda\, Ra\, Da\, \theta \mathbf{k} - \mathbf{V} - \frac{Fs}{\lambda Pr}|\mathbf{V}|\mathbf{V} + \Lambda\, Da\nabla^2 V \tag{5}$$

$$S\frac{\partial \theta}{\partial t} + (\mathbf{V}\cdot\nabla)\theta = \nabla^2\theta. \tag{6}$$

The governing parameters for the buoyancy-driven flow in porous media are thus:

fluid Rayleigh number, $Ra = g\beta D^3 \Delta T/\nu_f \alpha_f$ (7)

fluid Prandtl number, $Pr = (\nu/\alpha)_f$ (8)

Darcy number, $Da = K/D^2$ (9)

Forchheimer number, $Fs = b/D$ (10)

conductivity ratio, $\lambda = k_f/k_m$ (11)

viscosity ratio, $\Lambda = \mu'/\mu_f$ (12)

specific heat ratio, $S = (\rho c)_m/(\rho c)_f$ (13)

and the porosity, ε.

It is evident that the steady-state free convection in porous media is governed by seven basic parameters, *Ra* (or *Gr*), *Pr*, *Da*, *Fs*, λ, Λ and ε. Here *Ra* and *Pr* are functions of the thermophysical properties of the fluid, and do not depend on the porous matrix structure or its material properties. On the other hand, *Da*, *Fs* and ε generally depend on the porous matrix structure and its confinement, and only in a few special cases, are they influenced by the properties of the solid and fluid. However, λ and Λ are functions of both the solid and fluid thermophysical properties, and may also be governed by the hydrodynamic and thermal dispersion. It should also be noted that the porosity will not appear as an explicit parameter in equations (7)–(9) if the transport term, $(\mathbf{V}\cdot\nabla)\mathbf{V}$ is of low order of magnitude thus reducing the number of parameters to only six. In the case of a vertical cavity a geometrical parameter, the aspect ratio, A, also needs to be considered. It should be noted that most of the works on non-Darcy convection consider $\Lambda = 1$, i.e. $\mu' = \mu_f$. However, the variation in Λ is not fully understood, and, hence, the viscosity ratio has been considered as an independent parameter in the present study.

Another parameter of special attention is the Forchheimer number. Generally, the heat transfer investigators have either considered it as equal to $C\,Da^{0.5}$ or combined it with Ra^* to define a new modified Rayleigh number. Only Catton and co-workers [15, 16], and Prasad and Tuntomo [9] considered it as an independent parameter. However, Catton and co-workers used a similar parameter but combined it with *Pr* to obtain an effective Prandtl number. Since both *Fs* and *Da* are complex functions of ε, d and D, the relation $Fs = C\,Da^{0.5}$ is applicable only for a few selected conceptual models such as the Ergun model to represent the porous structure. Moreover, even for such models, $C = C(\varepsilon)$, and it can be taken as a constant only for a few special cases, e.g. a porous bed of spherical beads, $0.35 \leqslant \varepsilon \leqslant 0.45$. For $\varepsilon \cong 0.4$, C is obtained as 0.55, a value used by Beckermann *et al.* [12]. The motivation behind the present formulation is thus evident. The main advantage of this approach is that the effects of solid and fluid properties, and the porous matrix structure can be examined in a more rigorous way.

For two-dimensional natural convection in a vertical porous cavity the one vertical wall of which is isothermally heated at T_h, the other vertical wall is cooled at constant temperature T_c, and the horizontal walls are adiabatic, the governing equations (4)–(6) may be written in the stream function–vorticity form as

$$\nabla^2\psi = -\xi \tag{14}$$

$$\frac{Da}{\lambda Pr}\left[\frac{1}{\varepsilon}\frac{\partial\xi}{\partial t}+\frac{1}{\varepsilon^2}\left(u\frac{\partial\xi}{\partial x}+v\frac{\partial\xi}{\partial y}\right)\right] = -\xi+\Lambda Da\nabla^2\xi-\frac{Fs}{\lambda Pr}|\mathbf{V}|\xi + \frac{Fs}{\lambda Pr}\left(v\frac{\partial|\mathbf{V}|}{\partial x}-u\frac{\partial|\mathbf{V}|}{\partial x}\right)+\lambda Ra Da\frac{\partial\theta}{\partial x} \tag{15}$$

$$S\frac{\partial\theta}{\partial t}+u\frac{\partial\theta}{\partial x}+v\frac{\partial\theta}{\partial y}=\frac{\partial^2\theta}{\partial x^2}+\frac{\partial^2\theta}{\partial y^2}. \tag{16}$$

The relevant thermal boundary conditions for the present problem are

$$\theta = 0.5 \quad \text{at} \quad x = 0; \quad \theta = -0.5 \quad \text{at} \quad x = 1 \tag{17a}$$

$$\frac{\partial\theta}{\partial y} = 0 \quad \text{at} \quad y = 0, A. \tag{17b}$$

No-slip boundary conditions are applied for the velocity.

4. NUMERICAL METHOD

In this section we discuss the numerical method used for solving the governing equations (14)–(16). As it has been shown in the previous analytical and numerical studies, solutions of the Darcy–Brinkman equations exhibit viscous sublayers adjacent to the impermeable walls the thicknesses of which decrease when Ra increases or Da decreases. For example, using the boundary layer solution presented by Tong and Subramanian [10], the velocity peaks along the vertical walls are found to be located at a distance of the order of 2×10^{-2} for $Ra = 10^7$, $Da = 10^{-4}$ and $A = 1$ ($\lambda = \Lambda = 1$). When decreasing Da to 10^{-6} this distance is reduced to 10^{-3}. Similar effects were obtained in the numerical study given in ref. [11] for a larger range of Ra. Therefore, as a result of imposing no-slip boundary conditions in porous media, steep velocity gradients exist near the walls in the convection regimes provided Da is small. Thus, when solving the momentum equation by discrete methods such as finite difference methods (Taylor series expansions as well as control volume formulation) or finite element methods, a large number of mesh points are required near the walls in order to adequately resolve the flow field. If we consider that at least three mesh points have to be located between the walls and the velocity peaks, we obtain a mesh size of the order of 10^{-4} in the horizontal direction for Ra and Da of 10^{12} and 10^{-8}, respectively. In addition, since the velocity profile in the core region follows the classical Darcy profiles at low Darcy numbers, such small mesh sizes are useless and produce accumulation of rounding errors in the largest part of the flow field. Hence variable sized grids must be used to predict the flow and temperature fields accurately. However, as it has been shown in the literature, abrupt changes in mesh size leads to numerical instabilities and inaccuracies [17]. Consequently, numerical simulations at low Da systematically require the use of quite large numbers of mesh points.

In this study, coordinate transformations have been introduced for increasing the resolution in the viscous sublayers because this method is generally more accurate than mesh changes [17]. Accordingly, the x- and y-coordinates are transformed using an exponential stretch following the procedure described in an earlier publication [11]. The transformed equations were discretized using central differences for all spatial derivatives and the time integration was performed with an ADI algorithm and a false transient procedure. This solution technique is well described in the literature and has been widely used for natural convection in recirculating flows.

Concerning the Darcy–Brinkman part of the vorticity equation, some difficulties were encountered in implementing the boundary conditions at low Darcy numbers in the boundary layer regime. This is due to the steep velocity gradients near the walls which lead to numerical instabilities when using a second-order accurate formulation for the vorticity. Therefore, it was decided to employ the Thom first-order form. The Forchheimer term was split into two parts. The first part was combined with the Darcy term and numerically treated as an unknown with a non-linear coefficient. The other part, involving first-order derivatives of the velocity modulus as well as the buoyancy term, was modeled as a source term.

The steady state was assumed to be reached when the following convergence criterion was satisfied:

$$\sum_{i,j}|f_{ij}^{n+1}-f_{ij}^{n}|\Big/\sum_{i,j}|f_{ij}^{n}| < r_f \tag{18}$$

where n denotes the number of time increments. The residue r_f was taken as 10^{-4} for ψ and 5×10^{-6} for both ξ and θ. Further details of the computational method are omitted here for brevity, and may be found in our previous paper [11]. Comparison with numerical results based on the pure Darcy formulation and the Darcy–Forchheimer formulation were shown in previous papers [9, 11]. Therefore, the present predictions were compared only with the results reported recently by Beckermann *et al.* [12] for the Brinkman–Forchheimer–extended Darcy formulation. For the lowest Darcy numbers, the present calculations were made with as small grid sizes as 101×101. Table 1 shows that the present results are in good agreement with the Darcy–Brinkman solutions ($C = 0$) obtained by Beckermann [18] while larger

Table 1. Present Nusselt numbers compared with those represented by Beckermann [18]

Case	Ra	Da	Pr	$C = 0$ Present	$C = 0$ Ref. [18]	$C = 0.55$ Present	$C = 0.55$ Ref. [18]
1	10^5	10^{-1}	1	4.68	4.72	4.36	4.39
2	10^5	10^{-1}	0.01	4.68	4.72	1.94	1.94
3	10^8	10^{-4}	1	25.70	24.97	18.40	20.59
4	10^8	10^{-4}	0.01	25.70	24.97	6.19	6.02
5	10^{12}	10^{-8}	1	47.80	48.90	44.30	47.82
6	10^{12}	10^{-8}	0.01	47.80	48.90	21.50	19.45

discrepancies are seen for the Darcy–Brinkmann–Forchheimer model ($C = 0.55$) and high heat transfer rates. However, it should be noted that much coarser grids were used in ref. [18].

4. RESULTS AND DISCUSSION

To investigate properly the significance of Forchheimer's and Brinkman's modifications of the Darcy flow model, the numerical results have been obtained for wide ranges of governing parameters. First the Darcy–Brinkman solutions are re-examined. Next, the importance of the Forchheimer term is discussed, and finally, both the inertia and viscous diffusion effects are considered simultaneously.

4.1. *Re-examination of Darcy–Brinkman solutions*

4.1.1. *Effects of Darcy number.* To demonstrate the true effects of the fluid Rayleigh number and the Darcy number, the Darcy–Brinkman solutions for $A = 1$ and 5 are presented in Figs. 1 and 2 and Table 2, respectively. Although the solutions for negligible inertia forces are governed by only two groups of dimensionless parameters, $(\lambda Ra)/\Lambda$ and ΛDa, it is more convenient to look at these results for the case of $\lambda = \Lambda = 1$, particularly when we want to compare them with the fluid solutions.

Since an increase in Ra characterizes the enhancement in buoyant forces, the Nusselt number must increase with the fluid Rayleigh number. The slope then remains almost constant as long as the boundary layer flow is maintained in the Darcy regime as shown in Fig. 1 for $\Lambda Da = 10^{-6}$. The heat transfer correlations for such flow conditions are widely reported in the literature, e.g. $\overline{Nu} = C(\lambda Ra\, Da)^n A^{-m}$ where the values of the exponents n and m are very close to 0.5 for tall enough cavities. However, when Ra is increased beyond a value which delimits the Darcy regime, the slope of the Nusselt curve starts decreasing. This is quite evident from the curve for $Da = 10^{-4}$ in Fig. 1, which shows a reduction in slope from 0.6 at $Ra \cong 2 \times 10^6$ to 0.4 at $Ra \cong 7 \times 10^6$. The slope of this curve will further decrease and finally approach that for the pure fluid at Rayleigh number higher than 10^8. This has been clearly demonstrated by the experimental data of Seki *et al.* [19] for a vertical cavity, and of Prasad *et al.* [5] for a vertical annulus packed with large balls.

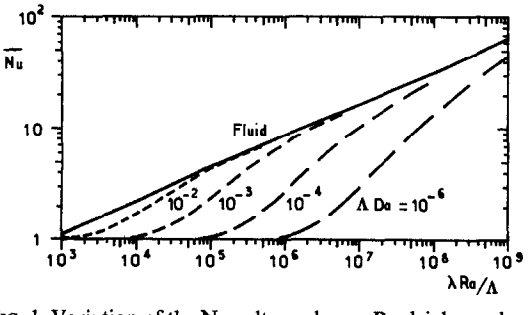

FIG. 1. Variation of the Nusselt number vs Rayleigh number for Darcy–Brinkman model ($A = 1$).

The above change in slope for the Nu curve can be observed only if the Darcy number is low, say $Da < 10^{-4}$. Otherwise, the slope starts decreasing long before it reaches a value close to 0.6, and approaches the fluid value, as shown by the Nusselt number curve for $Da = 10^{-2}$ in Fig. 1. Indeed, the present Nu curve merges with the fluid line when $Da = 10^{-2}$ and $Ra > 3 \times 10^5$.

Hence, in the non-Darcy regime, the slope of the Nusselt number curve decreases with an increase in ΛDa, and finally approaches zero (Fig. 2). The Darcy–Brinkman solutions thus show the existence of an asymptotic convection regime where the heat transfer rate is independent of the Darcy number or the permeability of the porous matrix, and depends only on the fluid Rayleigh number, and the conductivity and viscosity ratios. The higher the Rayleigh number, the earlier this asymptotic convection regime starts in terms of Da. It should also be noted that in the non-Darcy regime, the Darcy–Brinkman model predicts lower heat transfer rates than that obtained by employing the Darcy model (Fig. 2); the variation between the two Nusselt numbers increases with both $(\lambda Ra)/\Lambda$ and ΛDa.

It is further possible to use Fig. 2 to develop a plot for critical values of $(\lambda Ra)/\Lambda$ as functions of ΛDa, to delimit the conduction and the Darcy convection regimes. Figure 2 shows that the Darcy model is generally valid in the conduction flow regime, and hence the criterion developed by Prasad and Kulacki [20]

$$(\lambda Ra)/\Lambda = 10.7/(\Lambda Da), \quad A = 1 \qquad (20)$$

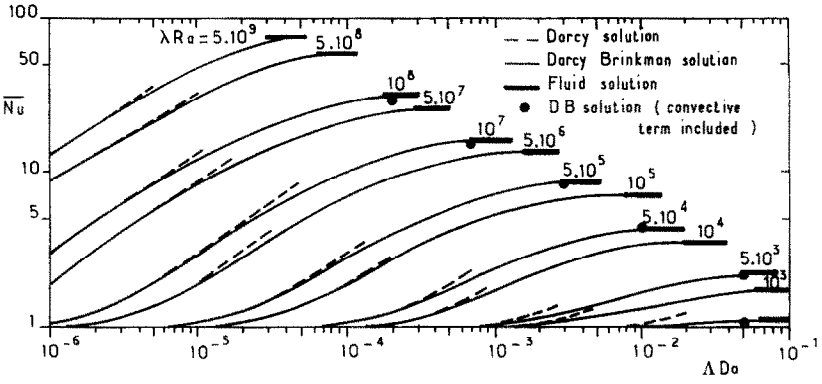

FIG. 2. Effect of Darcy number on the heat transfer rate at various Rayleigh numbers for a square vertical cavity.

may be used to delimit the conduction flow regime. This produces a straight line in Fig. 3.

A criterion in terms of 5% deviation from the Darcy solution leads to a delimiting curve for the Darcy regime as shown in Fig. 3. It can now be observed that the curves for conduction and Darcy regimes converge as the Darcy number increases indicating that the Darcy flow regime is highly restricted at large values of Da. On the other hand, the range for which the Darcy model is valid increases exponentially as the Darcy number is reduced. The criterion for the asymptotic convection regime to start is presented in Fig. 3 which shows that the gap between the curves for Darcy–Brinkman and asymptotic convection regimes decreases as ΛDa increases. On the other hand, the curves seem to be almost parallel for $\Lambda Da > 10^{-4}$. It is also interesting to note that the asymptotic convection is achieved within a two orders-of-magnitude increase in ΛDa from the start of the Darcy–Brinkman regime.

For $\lambda = 1$, the asymptotic Nusselt number for a fixed Ra is very close to the heat transfer rate in a fluid-filled cavity (Fig. 2 and Table 2) and hence, the asymptotic convection regime may be referred to as the fluid regime when $k_s = k_f$ and $\mu \simeq \mu'$. As one would expect, this asymptotic variation in Nusselt number is a direct consequence of appropriate modifications in the temperature and flow fields with the Darcy number. To show the asymptotic variation in θ and ψ fields, the isotherms and streamlines for $(\lambda Ra)/\Lambda = 10^6$ and $\Lambda Da = 10^{-5}$, 10^{-4}, 10^{-3} and 3×10^{-3} are presented in Figs. 4(a)–(d). It can now be observed that the flow intensity increases with the Darcy number, and a highly stratified medium with almost parallel, horizontal flow in the core is produced at $\Lambda Da > 10^{-3}$. Also, the striking similarity between the temperature and velocity fields for the porous medium at $(\lambda Ra)/\Lambda = 10^6$, $\Lambda Da = 3 \times 10^{-3}$ and that for the fluid at $Ra = 10^6$ ($Pr = 5$) in Figs. 4(d) and (e), respectively, can be easily noticed. This asymptotic trend is also demonstrated to some extent by the boundary layer solution of Tong and Subramanian [10] for a vertical cavity.

4.1.2. *Effect of conductivity ratio.* The present numerical results further show that the effect of conductivity ratio, λ, on the Darcy–Brinkman solutions is not straightforward. In the conduction regime, as one would expect, the heat transfer rate increases with the thermal conductivity of either the solid or the fluid or both. To demonstrate properly the effects of the conductivity ratio in other flow regimes, the Nusselt numbers for $\Lambda Da = 10^{-6}$, 10^{-4} and 10^{-2} and $\lambda = 0.01$, 0.1 and 1 are plotted in Fig. 5 in terms of the fluid Rayleigh number. These curves clearly show that for a given fluid, the heat transfer rate monotonically increases with the thermal conductivity of the solid particles, k_s, which increases the effective thermal conductivity of the porous medium, k_m, and

Table 2. Selected values of Nusselt number, Nu, for $A = 5$ compared to fluid results for $P = 5$ [23]

Ra	10^9	10^8	10^7	10^6	10^5	10^4	10^3
Da	3×10^{-4}	10^{-3}	6×10^{-3}	5×10^{-2}	10^{-1}	5×10^{-1}	5×10^{-1}
Porous	38.7	21.4	12.1	6.83	3.76	2.07	1.09
Fluid	38.9	21.9	12.3	6.92	3.89	2.09	1.09

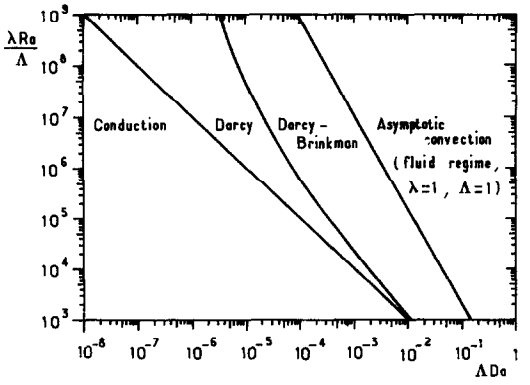

FIG. 3. Criteria to delimit the Darcy, Darcy–Brinkman and asymptotic regimes for a square vertical cavity.

reduces the conductivity ratio, λ. The variation is a maximum in the conduction regime, and becomes almost constant when the boundary layer flow is fully established.

Another important feature of Fig. 5 is the fact that the porous medium may transport a significantly larger amount of energy compared to the corresponding fluid medium. This is true for all flow regimes, but requires that the porous matrix be highly permeable (large Da) and $k_s > k_f$, and has been demonstrated clearly by the curves for $\Lambda Da = 10^{-4}$ and 10^{-2}. Even though a similar behavior can be demonstrated by the Darcy solution, no effort was made in the past, to the authors' knowledge, to understand fully this important property of the porous medium which may be utilized effectively to enhance the energy transport in heat exchange systems.

4.1.3. *Effect of viscosity ratio.* An increase in Λ reduces the Nusselt number by enhancing the contribution of the viscous diffusion term. The numerical results for a vertical cavity indicate that in the practical range of $0.5 < \Lambda < 2.5$, the variation in the viscosity ratio has little influence on the Darcy–Brinkman solutions if $Da < 10^{-5}$ and $\lambda Ra\,Da < 1000$ (Table 3). The upper limit of $\lambda Ra\,Da$ for the dependence on Λ to be negligible, may further be increased ten-fold for every two orders of magnitude reduction in the Darcy number below 10^{-5}, and vice versa.

4.2. *Significance of Forchheimer's modifications*

The Darcy–Forchheimer solutions for a vertical cavity [7–9] show that the Nusselt number based on the stagnant thermal conductivity, $\overline{Nu}$, decreases with an increase in the ratio of Forchheimer and modified Prandtl numbers, Fs/Pr^*. Prasad and Tuntomo [9] obtained the following heat transfer correlation for boundary layer flow:

$$\overline{Nu} = C_1\, Gr^{*p}\, Pr^{*q}\, Fs^{-r}\, A^{-s},$$

$$(p+r) \simeq 0.5, \quad q \simeq 0.5 \quad \text{and} \quad s \simeq 0.5 \qquad (21)$$

where $Gr^* = Gr\,Da$ is the Darcy-modified Grashof number.

The most interesting observation is that the exponent p decreases from 0.5 in the Darcy regime to 0.25 in the inertial flow regime. Consequently, r increases from 0 to 0.25. On the other hand, the dependence on the modified Prandtl number and the aspect ratio remains unaltered with the inclusion of the inertia term. It will now be interesting to examine the influence of the viscous diffusion effects on this behavior.

To end this section, it is worth noting that an opposite effect of Fs is found for packed-sphere beds. Indeed, the Ergun model shows that an increase in Forchheimer number is generally associated with an increase in the permeability of the porous matrix. Therefore, the Nusselt number should be expected to increase with Fs. This will become evident if we can combine the Darcy and Forchheimer numbers in equation (21) through the description of the porous matrix. For the Ergun model ($Fs = C\,Da^{0.5}$), we obtain

$$\overline{Nu} = C_2 \lambda^q\, Gr^p\, Pr^q\, Fs^{1-3r}\, A^{-s}. \qquad (22)$$

It is now easy to see that the heat transfer rate always increases with the Forchheimer number since $(1-3r)$ is a positive number. However, in the non-Darcy regime ($r > 0$), the Darcy–Forchheimer model predicts lower heat transfer rates than the Darcy formulation. Table 4 further shows that the higher the Rayleigh, Darcy and/or Forchheimer numbers, the larger is the difference between the two predictions.

As noted earlier, the Darcy–Brinkman solutions are valid only if $Fs/(\lambda Pr) \to 0$. In terms of the criteria developed in ref. [9], the Darcy flow limit is restricted

Table 3. Effects of the viscosity ratio, Λ, on mean Nusselt number for $A = 1$ (Darcy–Brinkman model)

	$Da = 10^{-7}$			$Da = 10^{-5}$			$Da = 10^{-3}$		
					λRa				
Λ	10^9	10^{10}	5×10^{10}	10^6	10^7	10^8	10^4	10^5	10^6
0.5	3.09	13.41	32.10	1.07	3.04	12.80	1.06	2.57	9.28
1	3.08	13.35	31.94	1.07	3.02	12.42	1.05	2.41	7.29
2	3.08	13.29	31.72	1.07	2.96	11.90	1.05	2.26	6.35

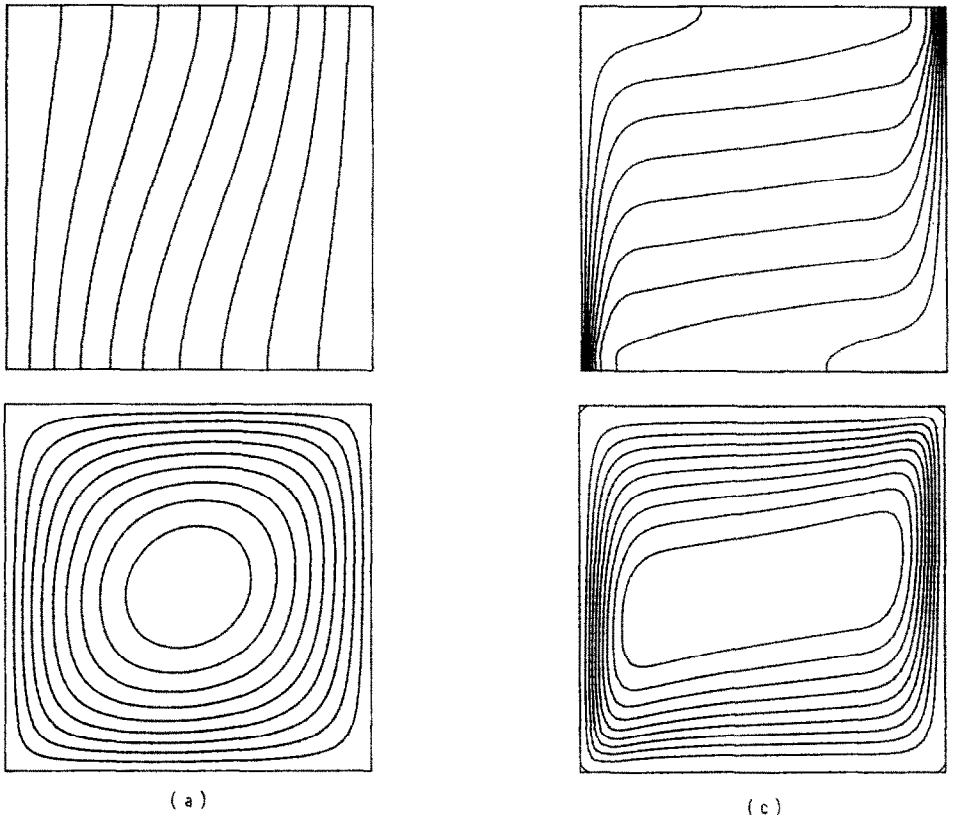

FIGS. 4(a)–(d).

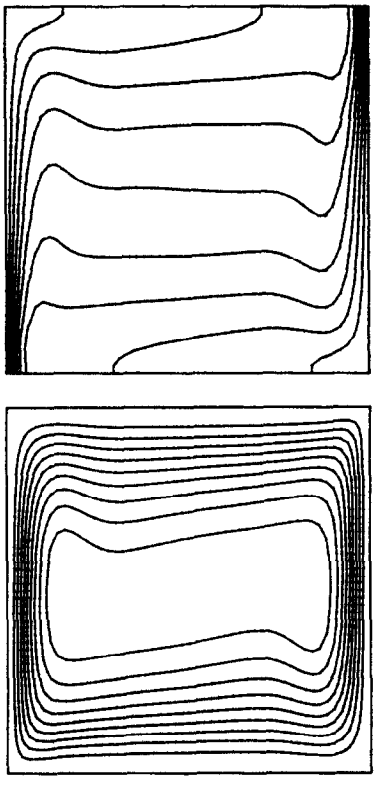

(e)

FIG. 4. Isotherms and streamlines for free convection in a square cavity for $(\lambda Ra)/\Lambda = 10^6$: (a) $\Lambda Da = 10^{-5}$; (b) $\Lambda Da = 10^{-4}$; (c) $\Lambda Da = 10^{-3}$; (d) $\Lambda Da = 3 \times 10^{-3}$; (e) fluid filled cavity with $Pr = 5$.

to

$$Fs > \begin{cases} 0.01/(Gr\,Da) & \varepsilon \to 0 \\ 0.1/(Gr\,Da) & \varepsilon = 0.9 \end{cases} \quad \text{for } Re_d = 1. \qquad (23)$$

Figure 2 shows that at least for the Ergun model, the Forchheimer term becomes important long before the contribution of the Brinkman term is of any significance. For example, the above criterion (23) predicts the inertial flow at $Ra \simeq 10^7$ and 10^4 for $Da = 10^{-6}$ and 10^{-4} ($\lambda Pr = 1$, $\varepsilon = 1$), respectively. These values of fluid Rayleigh number are much smaller than that required for the Darcy–Brinkman regime (Fig. 3). Clearly, any consideration of non-Darcy effects requires both the Forchheimer and Brinkman terms to be considered simultaneously.

4.3. *Darcy–Brinkman–Forchheimer solutions*

In this section, we shall present the Darcy–Brinkman–Forchheimer solutions in order to examine the combined effects of the Brinkman viscous diffusion and the Forchheimer inertia terms. The numerical results for a square cavity will be presented first and the effect of the aspect ratio will be considered later.

4.3.1. *Combined effects of Brinkman and Forchheimer terms.* Figure 6 shows that the inclusion of both Brinkman and Forchheimer terms in the equation of motion results in lower heat transfer rates than the Darcy solution at a fixed Darcy-modified Rayleigh number, $Ra^* = \lambda\, Ra\, Da$. As expected, the differences between the Darcy and Darcy–Brinkman–Forchheimer solutions increase with Ra^* since the effects of viscous diffusion and inertia become increasingly important as the flow circulation is enhanced. It should, however, be noted that Fig. 6 does not translate the effect of Da as discussed previously, that is, the heat transfer rate increases with increasing Da. The curve for $Fs/(\lambda Pr) = 0$ only shows that the validity of the Darcy model is limited to $Ra^* < 10^2$ for $\Lambda Da = 10^{-4}$ and $A = 1$. On the other hand, Fig. 6 depicts properly the effect of inertia in porous media for which the Forchheimer number is a weak function of permeability. These predictions are in agreement with those discussed previously.

In Fig. 7 the Nusselt number is plotted against the fluid Rayleigh number, Darcy number and $Fs/(\lambda Pr)$. It appears then that the Nusselt number for a constant $Fs/(\lambda Pr)$ increases with the Darcy number or ΛDa, which is consistent with the trends displayed by the Darcy–Brinkman solutions ($Fs/(\lambda Pr) = 0$) earlier. Surprisingly, Table 5 indicates that the effect of Darcy

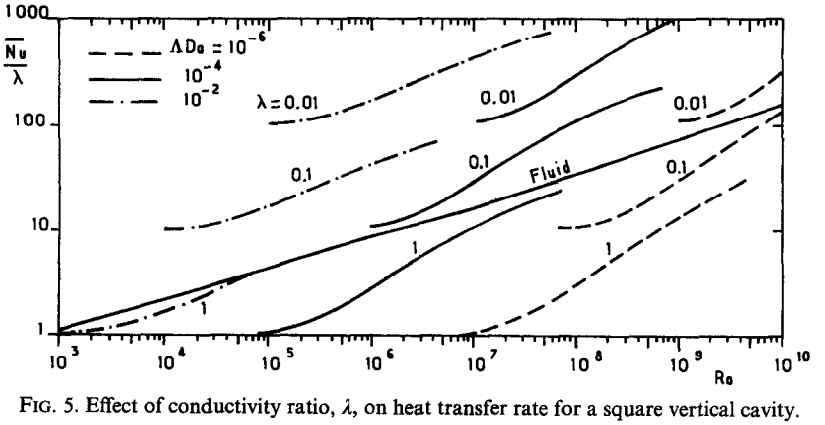

FIG. 5. Effect of conductivity ratio, λ, on heat transfer rate for a square vertical cavity.

Table 4. Nusselt numbers obtained from the Darcy–Brinkman and the Darcy–Forchheimer models ($Pr = 1$, $\Lambda = 1$)

		Darcy–Brinkman solution			Darcy–Forchheimer solution†	
Da	Ra	Darcy	($\Lambda = 1$)	$\varepsilon = 0.1$	$\varepsilon = 0.4$	$\varepsilon = 0.9$
10^{-6}	10^7	1.07	1.07	1.07	1.07	1.07
	10^8	3.09	3.06	3.01	3.07	3.09
	10^9	13.41	13.22	9.96	12.80	13.29
	5×10^9	32.13	31.50	17.90	26.15	29.60
10^{-4}	10^5	1.07	1.06	1.06	1.07	1.07
	10^6	3.09	2.84	2.35	2.97	3.05
	10^7	13.41	10.34	5.92	9.62	11.50
	5×10^7	32.13	20.85	10.02	17.20	21.70
10^{-2}	10^3	1.07	1.02		1.06	1.06
	10^4	3.09	1.70		2.28	2.67
	10^5	13.41	4.26		5.55	7.42
	5×10^5	32.13	7.10		9.60	13.10

† For Ergun model, $Fs = 0.143(Da/\varepsilon)^{0.5}$.

number is much stronger at higher values of $Fs/(\lambda\, Pr)$, that is, the stronger the inertia effects the more significant is the effect of $\Lambda\, Da$. For example, the enhancements in Nusselt number for an increase in $\Lambda\, Da$ from 2×10^{-4} to 10^{-3} at $Ra = 10^7$ are 29.4% at $Fs/(\lambda\, Pr) = 0$ and 41.8% at $Fs/(\lambda\, Pr) = 10^{-2}$. As can be expected, Table 5 shows also that the effect of $\Lambda\, Da$ is much stronger at high Rayleigh numbers.

Table 5 further shows that the inclusion of the inertia term in the equation of motion does not change the asymptotic behavior of the Nusselt vs Darcy number curve as displayed by the Darcy–Brinkman solution in Fig. 2. However, the stronger the Forchheimer inertia term, the larger is the Darcy number or $\Lambda\, Da$ required for the $\overline{Nu}$ curve to reach the asymptotic convection regime. Alternatively, for a fixed $\Lambda\, Da$, the Rayleigh number or $(\lambda\, Ra)/\Lambda$ at which the Darcy–Brinkman–Forchheimer solution will be independent of the permeability of the porous matrix or $\Lambda\, Da$, increases with $Fs/(\lambda\, Pr)$. This is a consequence of the diminishing boundary layer behavior with an increase in $Fs/(\lambda\, Pr)$.

It is now possible to modify Fig. 3 and present the criteria to delimit the non-Darcy flow regime in terms of $(\lambda\, Ra)/\Lambda$, $\Lambda\, Da$ and $Fs/(\lambda\, Pr)$ (Fig. 8). As can be expected, the extent of the Darcy regime reduces sharply with an increase in $\Lambda\, Da$ and/or $Fs/(\lambda\, Pr)$. On the other hand, the curve which delimits the asymptotic convection regime moves further away from the Darcy regime line with an increase in $Fs/(\lambda\, Pr)$. For $\lambda = \Lambda = 1$, the asymptotic convective state again represents the fluid regime (Table 5).

Although the numerical results have thus far been presented and discussed in terms of three groups of parameters, $(\lambda\, Ra)/\Lambda$, $\Lambda\, Da$ and $Fs/(\lambda\, Pr)$ in order to understand properly the significance of Brinkman's

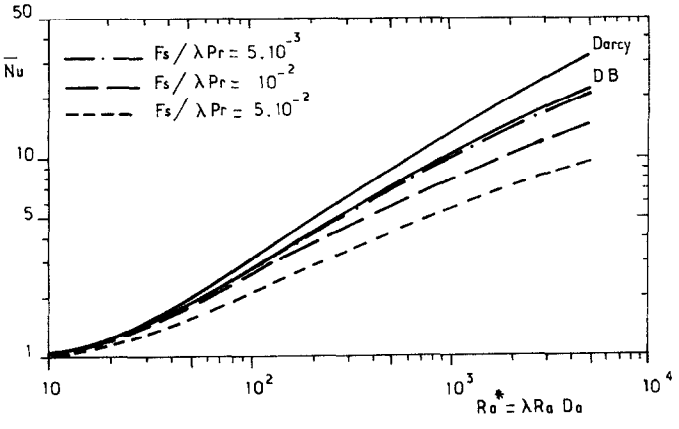

FIG. 6. Effects of inertia on the Nusselt number and comparison with Darcy and Darcy–Brinkman solutions ($A = 1$, $Da = 10^{-4}$, $\Lambda = 1$).

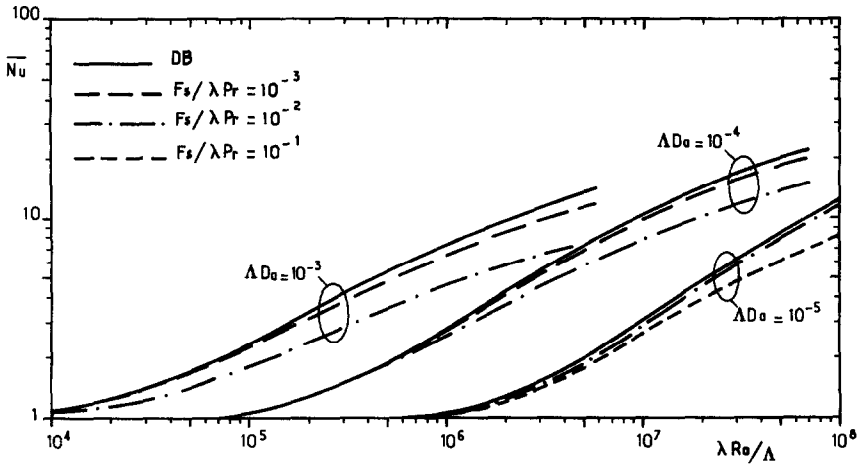

FIG. 7. Variation of the Nusselt number vs $(\lambda Ra)/\Lambda$ for a square vertical cavity.

and Forchheimer's modifications, it is not very difficult to interpret these results in terms of the fluid Rayleigh number, *Ra*, and the porous scaling parameters, *Da* and *Fs*. A simple substitution of $\lambda = \Lambda = Pr = 1$ can serve this purpose.

4.3.2. *Effects of conductivity ratio, Prandtl number and aspect ratio.* Since the advective terms in the momentum equation were found to be of low order of magnitude [11], the influence of conductivity ratio and Prandtl number can be deduced immediately from an examination of equation (5).

Concerning the effects of λ, it is clear that a decrease of λ yields simultaneously an increase of the inertia term and a decrease of the buoyancy force term. Therefore, the flow is slowed down and the Nusselt number based on stagnant thermal conductivity decreases. However, as for the Darcy–Brinkman solution, the ratio $\overline{Nu}/\lambda$, that is the fluid Nusselt number, increases with decreasing λ. This is evident from Figs. 6 and 7, and Table 5. Hence, the conclusions drawn in Section 4.1.2 are still valid.

An increase of *Pr* reduces the effect of inertia and thus enhances the heat transfer rate. Therefore, the Prandtl number could have a much higher influence on the mean Nusselt number than for pure fluid enclosures according to the porous matrix structure. Indeed, as it can be seen in Fig. 7, changes in *Pr* would weakly modify $\overline{Nu}$ for very low values of *Fs*, and ordinary fluids, i.e. $Fs < 10^{-4}$ and $Pr > 0.5$. On the other hand, an increase of *Pr* by an order of magnitude would have a much greater effect for a porous matrix with $Fs \simeq 10^{-3}$ (see Fig. 7). Therefore, it should be

Table 5. Effect of $(\lambda Ra)/\Lambda$, ΛDa and $Fs/(\lambda Pr)$ on the Nusselt number for $A = 1$ (fluid solutions for $Pr = 5$)

		ΛDa						
$(\lambda Ra)/\Lambda$	$Fs/(\lambda Pr)$	10^{-4}	5×10^{-4}	10^{-3}	5×10^{-3}	10^{-2}	2×10^{-2}	Fluid
10^5	0	1.07	1.78	2.45	3.94	4.31	4.53	4.70
	10^{-3}	1.07	1.77	2.43	3.92	4.29	4.52	
	10^{-2}	1.07	1.71	2.32	3.76	4.17	4.34	
		ΛDa						
		10^{-5}	5×10^{-5}	10^{-4}	5×10^{-4}	10^{-3}	3×10^{-3}	
10^6	0	1.08	1.93	2.91	6.21	7.44	8.72	9.22
	10^{-3}	1.08	1.92	2.88	6.09	7.32	8.58	
	10^{-2}	1.07	1.85	2.67	5.40	6.58	7.82	
		ΛDa						
		10^{-6}	5×10^{-6}	10^{-5}	5×10^{-5}	10^{-4}	5×10^{-4}	
10^7	0	1.08	1.98	3.08	8.09	10.94	16.28	17.35
	10^{-3}	1.08	1.97	3.04	7.78	10.44	15.66	
	10^{-2}	1.07	1.88	2.78	6.35	8.35	13.06	

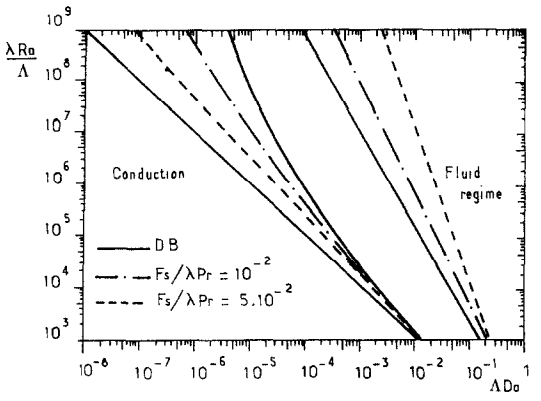

FIG. 8. Criteria to delimit the Darcy, Darcy–Brinkman–Forchheimer and asymptotic regimes for a square vertical cavity.

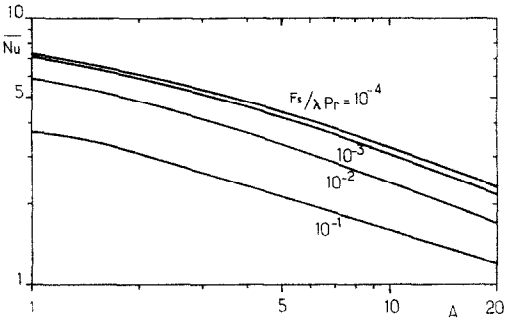

FIG. 10. Effects of cavity aspect ratio on Nusselt number ($\Lambda Da = 10^{-4}$, $(\lambda Ra)/\Lambda = 5 \times 10^6$).

pointed out here that no general trend could be drawn concerning the effect of Pr in porous media without specifying the matrix scaling parameters (Da and Fs for uniform porosity media). The effects of the Prandtl number for a packed-sphere cavity are illustrated in Fig. 9 for three dimensionless particle diameters ($\gamma = d/D$) and $Ra = 10^8$. Using the Ergun model, the Darcy number is found to be close to $Da = 5 \times 10^{-4}\gamma^2$ and we have assumed that $Fs = 0.55Da^{0.5}$ (i.e. $\varepsilon \cong 0.4$). Therefore, the problem formulation depends on three parameters only for a square cavity (Ra, Pr and γ). As can be seen, the Prandtl number has a small influence on the Nusselt number for $Pr > 0.1$ at $\gamma = 0.05$, and for $Pr > 1$ at $\gamma = 0.2$ which is the highest γ-value compatible with local-averaged equations. These results are in agreement with the numerical results reported by Beckermann *et al.* [12] and David *et al.* [21]. As in pure fluid enclosures, the Nusselt number increases with Pr. It should be emphasized that the critical values for neglecting the Pr dependence increase with increasing Ra and decrease with decreasing γ.

Finally, the dependence of the Nusselt number on aspect ratio was examined for $A \geqslant 1$. As the cavity becomes taller, Fig. 10 shows decreases of the heat transfer rate at constant and large enough Ra ($\Lambda Ra = 5 \times 10^6$), in agreement with the predictions of the boundary layer type analyses for Darcy and Darcy–Forchheimer models [7, 22]. Since the various curves for a wide range of $Fs/(\lambda Pr)$ are almost parallel for $A \geqslant 3$, it is thus evident that the effects of A are almost independent of the contribution of inertia and viscous diffusion, and are essentially controlled by the flow regimes. It should be noted that the solutions obtained in ref. [9] indicate a similar behavior. If a correlation $\overline{Nu} = cA^{-n}$ can be obtained, the exponent of A would depend upon the Rayleigh number unless the heat transfer rate is clearly dominated by convective effects. In that case, Weber's theory [22] predicts $n = 0.5$. The results reported in Fig. 10 lead to $n \simeq 0.46$ for $3 \leqslant A \leqslant 20$.

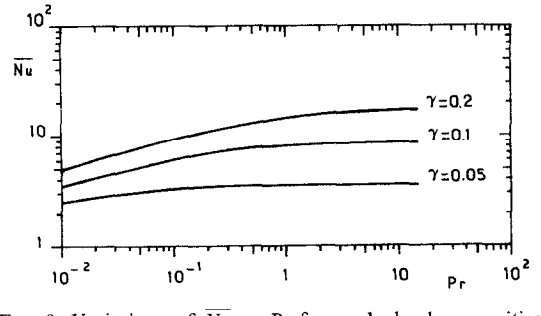

FIG. 9. Variations of $\overline{Nu}$ vs Pr for packed-sphere cavities with $A = 1$ ($Da = 5 \times 10^{-4}\gamma^2$, $Fs = 0.55Da^{-0.5}$, $Ra = 10^8$).

5. CONCLUSION

The effects of inertia and viscous forces on natural convection in vertical porous cavities have been investigated numerically. The results clearly show the importance of non-Darcian effects both on the heat transfer rate and the flow regime. Re-examination of the Darcy–Brinkman solutions shows that there exists an asymptotic convection regime where the heat transfer rate is independent of permeability of the porous matrix. In this regime, not only the Nusselt number but also the temperatures and flow fields match with the fluid solutions corresponding to $k_f = k_m$. This asymptotic regime is reached at lower fluid Rayleigh numbers with increasing permeability. The inclusion of the Forchheimer term in the momentum equation leads to a reduction of the heat transfer rate. Therefore, the values of Ra for the asymptotic convection regime are higher if inertia effects are important. Criteria to delimit the Darcy, Darcy–Brinkman–Forchheimer and asymptotic convection regimes are presented for a square cavity. It is shown that the validity for the Darcy model increases with a reduction in both Darcy and Forchheimer numbers.

Present results also indicate that the heat transfer rate increases with a reduction in the conductivity

ratio. The implication is that a porous medium can transport more energy than the saturating fluid alone if the thermal conductivity of the solid particles is higher than that for the fluid and the porous matrix is highly permeable.

For a fixed fluid Rayleigh number, the effects of Prandtl number depend mainly upon the porous matrix scaling parameters. In the range of Ra investigated, it may be concluded that significant Prandtl number effects are obtained in a square cavity provided $Fs > 10^{-3}$. On the other hand, the non-Darcian effects do not modify the well-established dependence of the Nusselt number on the cavity aspect ratio in the boundary layer regime.

Acknowledgments—The authors gratefully acknowledge the support of this work by the National Science Foundation, U.S.A. (Grant No. CBT 85-04100) and by CNRS-PIRSEM, France (Grant No. 86820N2052). The computational facilities provided by CRNS Computing Center (CIRCE) are highly appreciated.

REFERENCES

1. P. Cheng, Heat transfer in geothermal systems, *Adv. Heat Transfer* **14,** 1–105 (1978).
2. V. Prasad, F. A. Kulacki and M. Keyhani, Natural convection in a porous media, *J. Fluid Mech.* **150,** 89–119 (1985).
3. C. L. Tien and J. T. Hong, Natural convection in porous media under non-Darcian and non-uniform permeability conditions. In *Natural Convection* (Edited by S. Kakaç, W. Aung and R. Viskanta). Hemisphere, Washington, DC (1985).
4. P. Cheng, Wall effects on fluid flow and heat transfer in porous media. *Proc. ASME/JSME Heat Transfer Conf.*, pp. 297–303 (1987).
5. V. Prasad, G. Lauriat and N. Kladias, Reexamination of Darcy–Brinkman solutions for free convection in porous media, *Int. Symp. Convection in Porous Media: Non-Darcy Effects, Proc. 25th Nat. Heat Transfer Conf.*, Vol. 1, pp. 569–580 (1988).
6. N. Kladias and V. Prasad, Benard convection in porous media: effects of Darcy and Prandtl numbers, *Int. Symp. Convection in Porous Media: Non-Darcy Effects, Proc. 25th Nat. Heat Transfer Conf.*, Vol. 1, pp. 593–604 (1988).
7. D. Poulikakos and A. Bejan, The departure from Darcy flow in natural convection in a vertical porous layer, *Physics Fluids* **28,** 3477–3484 (1985).
8. D. Poulikakos, A departure from the Darcy model in boundary layer natural convection in a vertical porous layer with uniform heat flux, *J. Heat Transfer* **107,** 716–720 (1985).
9. V. Prasad and A. Tuntomo, Inertia effects on natural convection in a vertical porous cavity, *Numer. Heat Transfer* **11,** 295–320 (1987).
10. T. W. Tong and E. Subramanian, A boundary layer analysis for natural convection in porous enclosure: use of the Brinkman–extended Darcy model, *Int. J. Heat Mass Transfer* **28,** 563–571 (1985).
11. G. Lauriat and V. Prasad, Natural convection in a vertical porous cavity: a numerical study for Brinkman–extended Darcy formulation, *J. Heat Transfer* **11,** 295–320 (1987).
12. C. Beckermann, R. Viskanta and S. Ramadhyani, A numerical study of non-Darcian natural convection in a vertical enclosure filled with a porous medium, *Numer. Heat Transfer* **10,** 557–570 (1986).
13. J. Bear, *Dynamics of Fluids through Porous Media.* Elsevier, New York (1972).
14. T. S. Lundgren, Slow flow through random beds and suspension of spheres, *J. Fluid Mech.* **51,** 273–299 (1972).
15. T. Jonsson and I. Catton, Prandtl number dependence of natural convection in porous media, *J. Heat Transfer* **109,** 371–377 (1987).
16. J. G. Georgiadis and I. Catton, Prandtl number effect on Benard convection in porous media, *J. Heat Transfer* **108,** 284–290 (1986).
17. P. J. Roache, *Computational Fluid Dynamics.* Hermosa, Albuquerque, New Mexico (1982).
18. C. Beckermann, Personal communication (1988).
19. N. Seki, S. Fukusako and H. Inaba, Heat transfer in a confined rectangular cavity packed with porous media, *Int. J. Heat Mass Transfer* **21,** 985–989 (1978).
20. V. Prasad and F. A. Kulacki, Convection heat transfer in a rectangular porous cavity: effects of aspect ratio on flow structure and heat transfer, *J. Heat Transfer* **106,** 158–165 (1984).
21. E. David, G. Lauriat and P. Cheng, Natural convection in rectangular cavity filled with variable porosity media, *Proc. 1988 Nat. Heat Transfer Conf.*, Houston, Vol. 1, pp. 605–612 (1988).
22. J. E. Weber, The boundary layer regime for convection in a vertical porous layer, *Int. J. Heat Mass Transfer* **18,** 569–573 (1975).
23. N. Seki, S. Fukusako and H. Inaba, Heat transfer of natural convection in a rectangular cavity with vertical walls of different temperatures, *Bull. JSME* **21,** 246–253 (1978).

EFFETS DES EXTENSIONS DE LA LOI DE DARCY SUR LA CONVECTION NATURELLE DANS UNE CAVITE POREUSE VERTICALE

Résumé—L'importance relative des forces visqueuses et des forces d'inertie sur la convection naturelle en milieux poreux est étudiée dans le cas d'une cavité chauffée différentiellement en se basant sur la formulation de Darcy–Brinkman–Forchheimer. Les résultats numériques montrent qu'il existe un régime asymptotique pour lequel la solution devient indépendante de la perméabilité de la matrice poreuse et des nombres de Darcy et de Forchheimer. Ce régime est atteint pour des nombres de Darcy et de Forchheimer d'autant plus faibles que le nombre de Rayleigh, basé sur les propriétés physiques du fluide, est élevé. Lorsque les conductivités des deux phases sont identiques, le nombre de Nusselt global et la structure de l'écoulement sont alors proches de ceux obtenus dans un fluide à un même nombre de Rayleigh. En outre, le nombre de Nusselt basé sur la conductivité du fluide augmente toujours avec les nombres de Rayleigh et de Darcy et avec le rapport de la conductivité du solide à celle du fluide alors qu'il décroit lorsque Fs augmente. L'effet du nombre de Prandtl dépend du régime convectif et des valeurs des autres paramètres. Les solutions numériques montrent aussi que le flux de chaleur transféré peut être supérieur à celui calculé dans le cas d'un fluide lorsque la perméabilité de la matrice est suffisamment élevée et lorsque la conductivité thermique du solide est supérieure à celle du fluide. Les limites des différents régimes d'écoulement sont présentés graphiquement pour une cavité carrée.

NICHT-DARCY'SCHE EINFLÜSSE AUF DIE NATÜRLICHE KONVEKTION IN EINEM VERTIKALEN PORÖSEN BEHÄLTER

Zusammenfassung—Die relative Bedeutung der Trägheits- und Zähigkeitskräfte für die natürliche Konvektion in porösen Medien wurde mittels Darcy–Brinkman–Forchheimer-Lösungen für einen partiell beheizten vertikalen Behälter untersucht. Die Ergebnisse zeigen, daß es einen asymptotischen Konvektionsbereich gibt, in dem die Lösung unabhängig von der Permeabilität der porösen Matrix oder der Darcy-Zahl (*Da*) und der Forchheimer-Zahl (*Fs*) ist. Je höher die Rayleigh-Zahl des Fluids, *Ra*, ist, desto früher beginnt dieser Bereich. In diesem Stadium stimmt sowohl die mittlere Nusselt-Zahl als auch das Temperatur- und Strömungsfeld für eine bestimmte *Ra*-Zahl mit den Ergebnissen für das Fluid überein, sofern das poröse Medium dieselbe Wärmeleitfähigkeit wie das Fluid hat. Anderfalls steigt die *Nu*-Zahl mit der *Ra*-Zahl des Fluids, der *Da*-Zahl und dem Verhältnis der Wärmeleitfähigkeiten an, während sie mit steigender *Fs*-Zahl fällt. Der Effekt der Prandtl-Zahl ist nicht einfach und hängt vom Strömungsgebiet und anderen Parametern ab. Die numerischen Lösungen zeigen außerdem, daß es möglich ist, daß ein poröses Medium mehr Energie als das sättigende Fluid allein transportieren kann, wenn die poröse Matrix hochpermeabel und ihre Wärmeleitfähigkeit höher als die des Fluids ist. Es werden außerdem einige Kriterien zur Abgrenzung der unterschiedlichen Konvektionsgebiete für einen quadratischen Behälter dargestellt.

ВЛИЯНИЕ НА ЕСТЕСТВЕННУЮ КОНВЕКЦИЮ В ВЕРТИКАЛЬНОЙ ПОРИСТОЙ ПОЛОСТИ ФАКТОРОВ, НЕ УЧИТЫВАЕМЫХ ЗАКОНОМ ДАРСИ

Аннотация—С помощью решений Дарси–Бринкмана–Форшхаймера для неравномерно нагретой вертикальной полости сопоставляется влияние инерционных и вязкостных сил на естественную конвекцию в пористой среде. Полученные результаты указывают на существование асимптотического режима конвекции, при котором решение не зависит от проницаемости пористой матрицы, то ехть от чисел Дарси *Da* и Форшхаймера *Fs*. Чем больше число Рэлея *Ra* для жидкости, тем с меньших значений чисел *Da* и *Fs* проявляется этот режим. При указанном режиме не только среднее число Нуссельта, но также температурные и скоростные поля для фиксированного числа Рэлея согласуются с аналогичными результатами для жидкости, если отношение коэффициентов теплопроводности для пористой среды равно единице. В противном случае число Нуссельта всегда увеличивается с ростом числа Рэлея для жидкости, числа Дарси и отношения коэффициентов теплопроводности и уменьшается с ростом числа Форшхаймера *Fs*. Число Прандтля влияет на число Нуссельта косвенным образом через режим течения и другие параметры. Численные решения показывают, кроме того, что пористая среда может передавать большую энергию по сравнению с насыщающей жидкостью, если пористая матрица обладает большой проницаемостью, а коэффициент теплопроводности твердых частиц больше коэффициента теплопроводности жидкости. Сформулированы также некоторые критерии классификации режимов конвективного течения в полости квадратного сечения.